Geant4 Lunar Albedo Computed Environment (GLACE): A Freely-Available Model of Lunar Albedo and Its Variation with Regolith Hydrogen

M. D. Looper, J. E. Mazur, J. B. Blake, H. E. Spence, N. A. Schwadron, J. K. Wilson, A. P. Jordan, C. Zeitlin, A. W. Case, J. C. Kasper, L. W. Townsend, T. J. Stubbs, P. H. Phipps

December 6, 2023

Approved for public release. OTR 2023-01211

Lunar Energetic-Particle Secondary Radiation ("Albedo")

Simulations were initially devised to help understand LRO/CRaTER proton observations

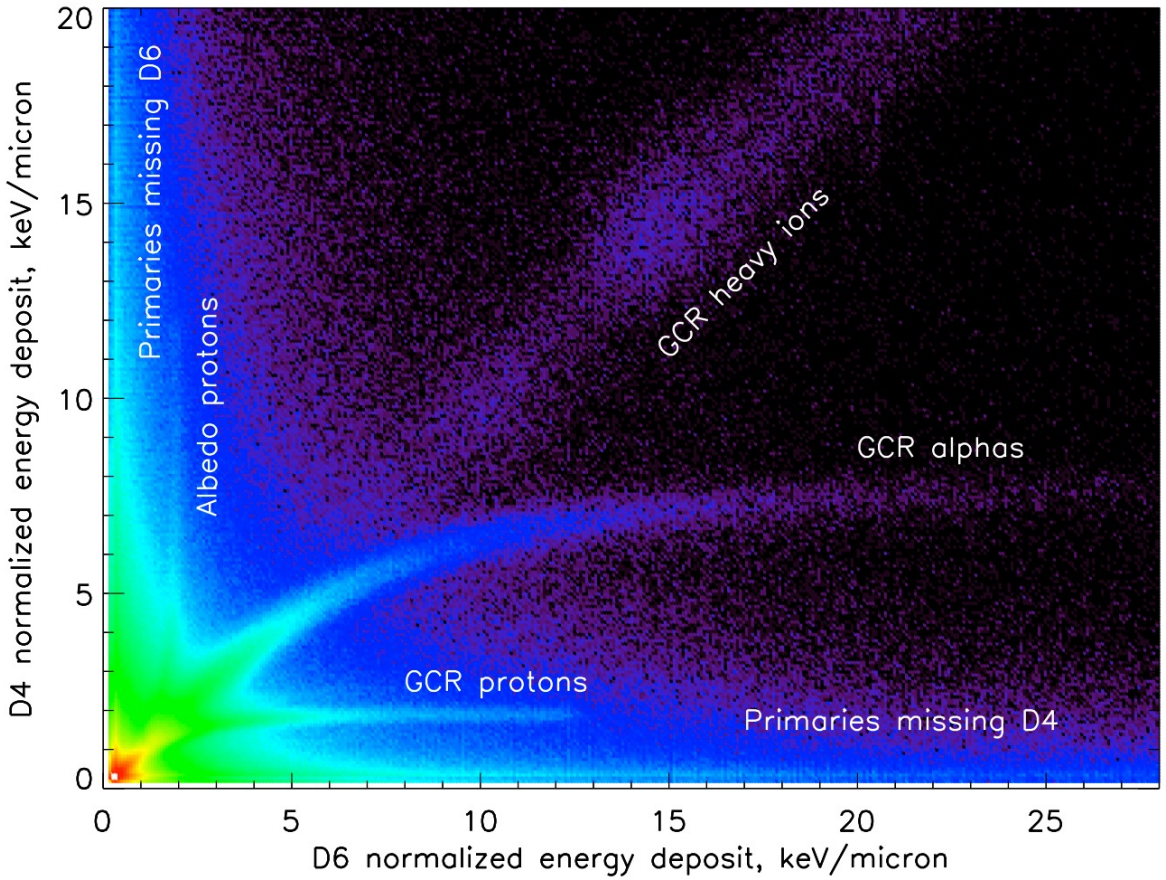

After Looper et al. (2013)

- Albedo particles are produced when cosmic-ray nuclei strike solar system bodies (e.g., atmosphere of Earth or surface of Moon).
- Cosmic Ray Telescope for the Effects of Radiation (CRaTER) sensor aboard Lunar Reconnaissance Orbiter (LRO) detected albedo protons (see left).
- Lunar Exploration Neutron Detector (LEND) aboard LRO and other instruments have measured albedo neutrons.
- Characteristics of albedo particles will vary depending on composition of surface struck by incident ions – in particular, this provides a means to sense water/ice remotely.
- Albedo particles are also of concern for the radiation exposure of astronauts and hardware at or near the lunar surface.

GLACE (Geant4 Lunar Albedo Computed Environment) Model

Freely-available encapsulation of hundreds of processor-years of Geant4 simulations

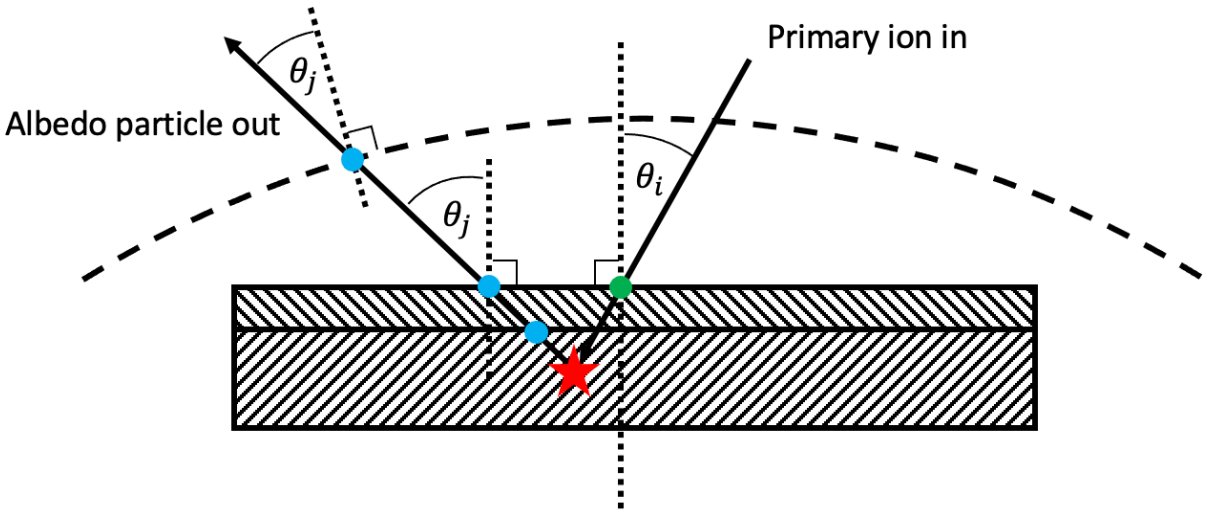

Primary model content is a set of "kernels" to allow calculation of energy/angle distributions of fluxes of γ, e-, e+, μ-, μ+, π-, π+, neutrons, ^{1}H, ^{2}H, ^{3}H, ^{3}He, ^{4}He, heavier isotopes of He, ions heavier than He, and all other miscellaneous subatomic particles (kaons, sigmas, etc.), as simulated using Geant4 (Allison et al., 2016).

- Isotropically incident monoenergetic ions H to Ni at 200 energies from 10 MeV/nuc to 10 GeV/nuc (to 100 GeV/nuc for incident protons)
- Sixteen target geometries: either dry ferroan anorthosite (FAN) or a layer of dry FAN topped by 1 mm, 1 cm, 10 cm, 1 m, or 10 m of FAN doped with 1% H, 10% H, or 9% H_2O (1% H and 8% O) by weight, total slab thickness 20 m
- Escaping particles tabulated at surface and at 20 km altitude above impact point (blue dots)
- Stored as JSON tabulations of normalized "kernels" $R_j(E_i, E_j, \theta_j)$ such that

$$J_j(E_j, \theta_j) = \int_0^\infty dE_i R_j(E_i, E_j, \theta_j) j_i(E_i)$$

- 96 zipfiles from 0.4 to 6 GB so a user need only download those needed for particular use case

Energy-Angular Distribution of Protons from Dry FAN, Solar Minimum

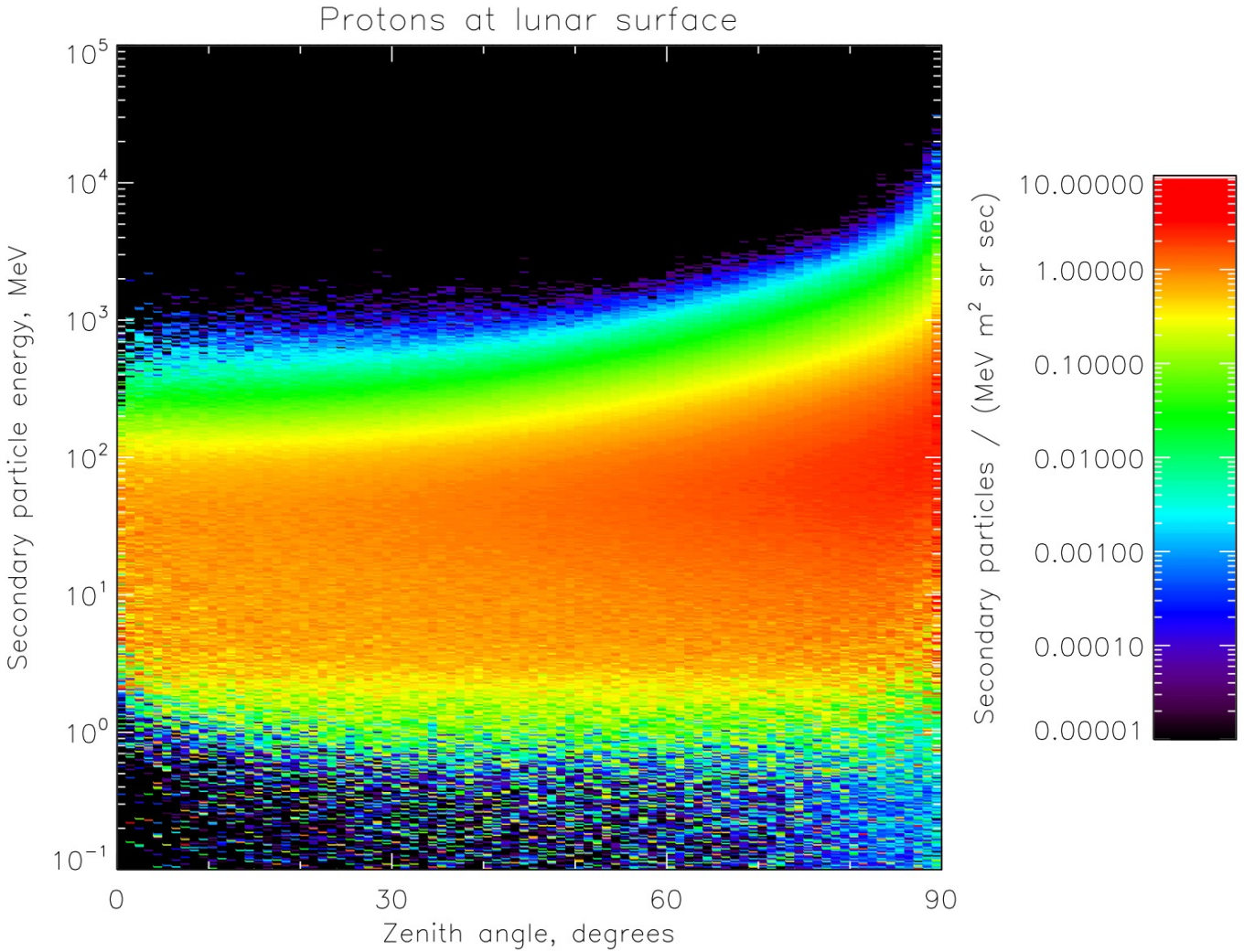

- GLACE distribution includes sample flux distributions (as JSON and PNG) for each species and geometry and for solar maximum and minimum modulation.
- Example at left shows protons escaping from the surface above a target of dry FAN when bombarded by solar-minimum ion spectra from Badhwar-O'Neill 2020 model (Slaba & Whitman, 2020).
- Colorscale is flux, and axes are secondary particle energy (600 bins) and angle of velocity away from zenithward (90 bins).
- Most species have near-isotropic distributions at lower energies (due to fragmentation of nuclei struck by cosmic rays down to a couple meters depth) and intensification/hardening toward the limb.

Energy-Angular Distribution of Neutrons from Dry FAN, Solar Minimum

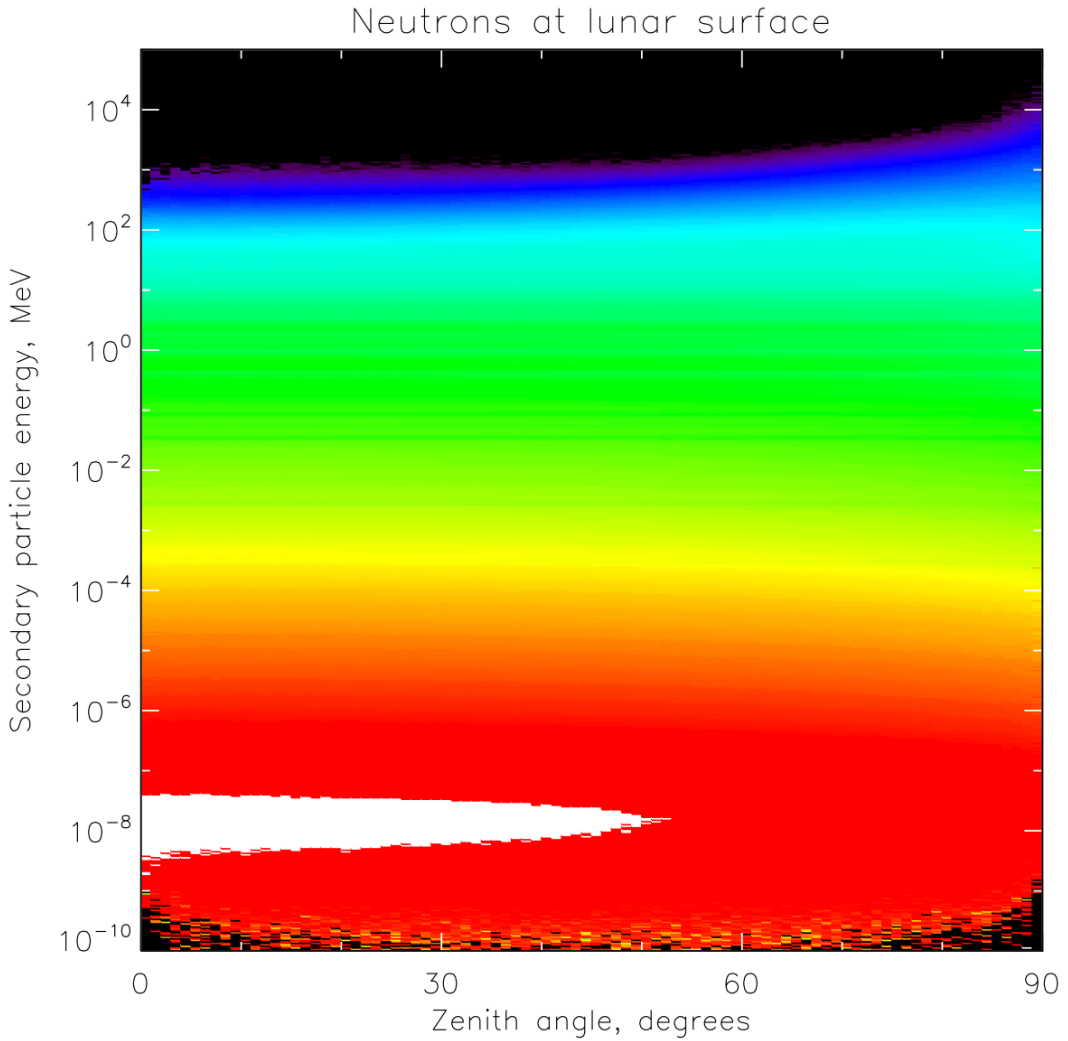

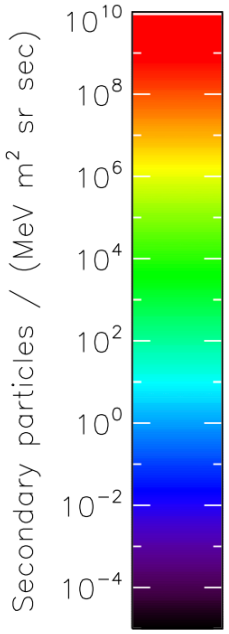

- This is the example energy/angle flux distribution for neutrons rising from the surface of a slab of dry FAN when bombarded by solar-minimum ion spectra.
- Note dynamic range of neutron energy (vertical scale) goes down to thermal energies, where protons and all other species stop at 0.1 MeV or MeV/nuc.
- Upgoing neutrons are also tabulated at boundary between dry and H/H_2O-bearing slabs (10 cm depth for entirely dry target) to study transfer of their energy to protons.

Effects of 1 cm Layer with 1% H on Albedo Protons (Solar Minimum)

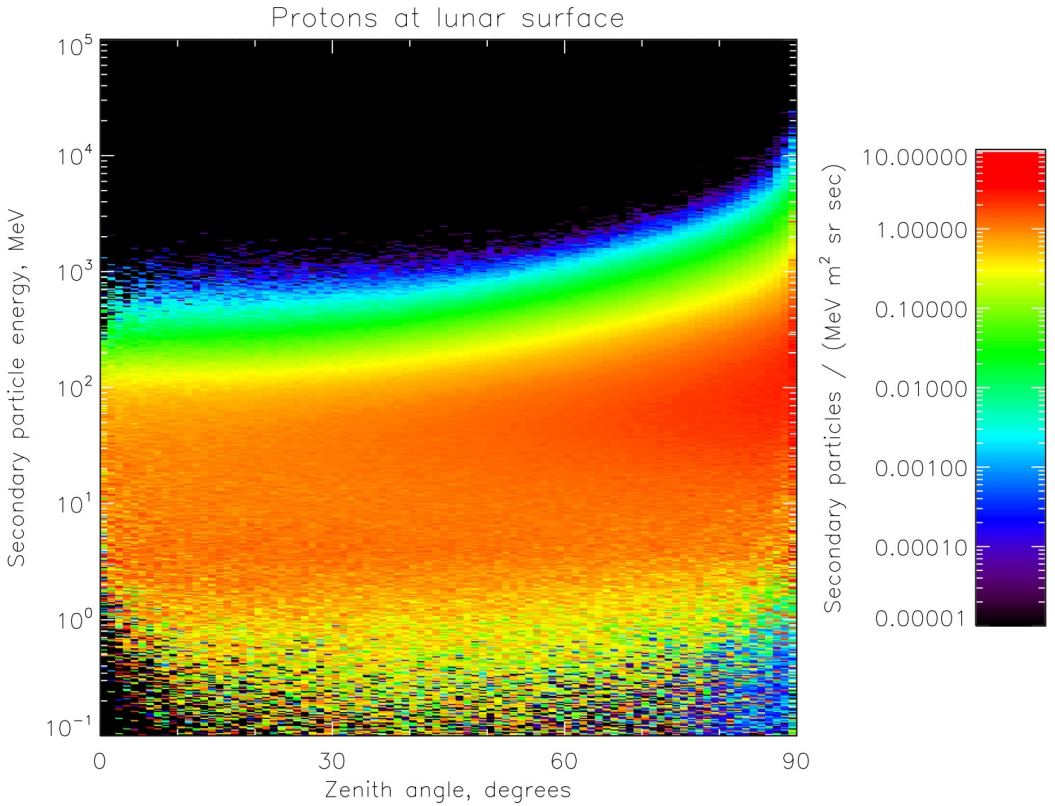

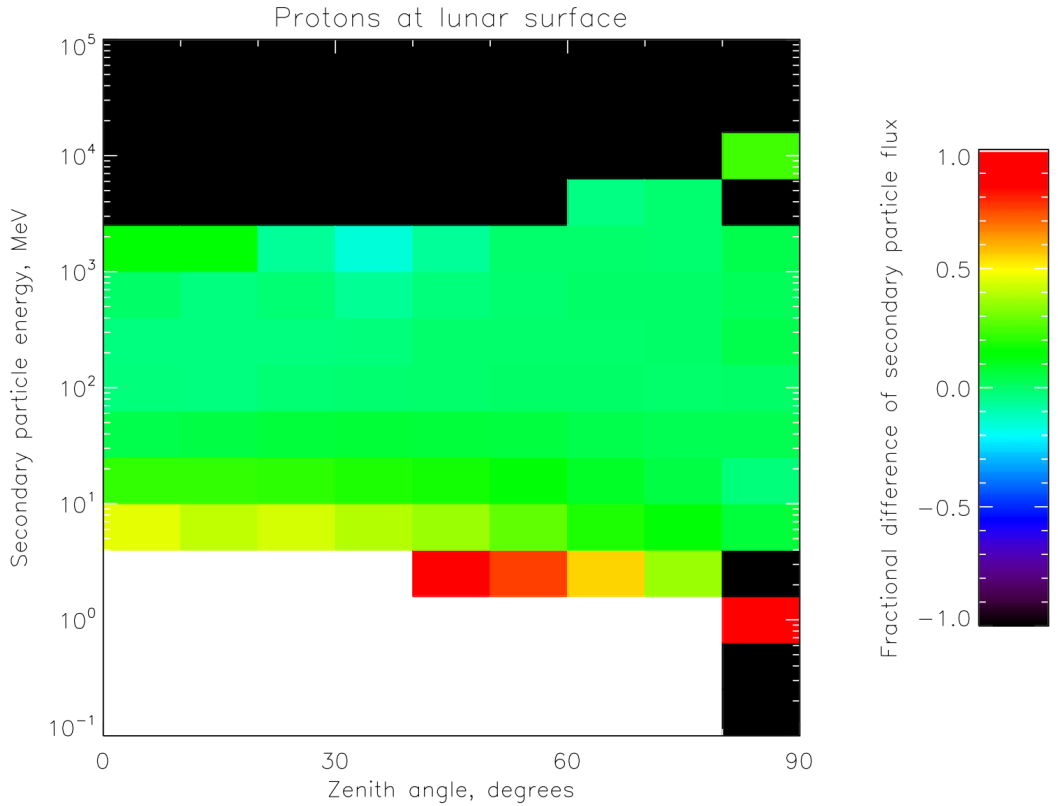

In the first iteration of this calculation (about 2018), protons were only tabulated down to 10 MeV, which is as low as CRaTER can sense (two-detector track on slide 2 is several tens of MeV and up). At left is sample file from the model distribution of albedo protons from solar minimum ion spectra striking a 1 cm layer with 1% of H by weight above dry FAN, and at right is difference file relative to dry FAN target on slide 4 (with resolution coarsened to give good statistics on the difference). Protons at CRaTER energies are depressed a few percent, but in the MeV range and below are substantially enhanced. (Black indicates poor statistics.)

Effects of 1 cm Layer with 1% H on Albedo Neutrons (Solar Minimum)

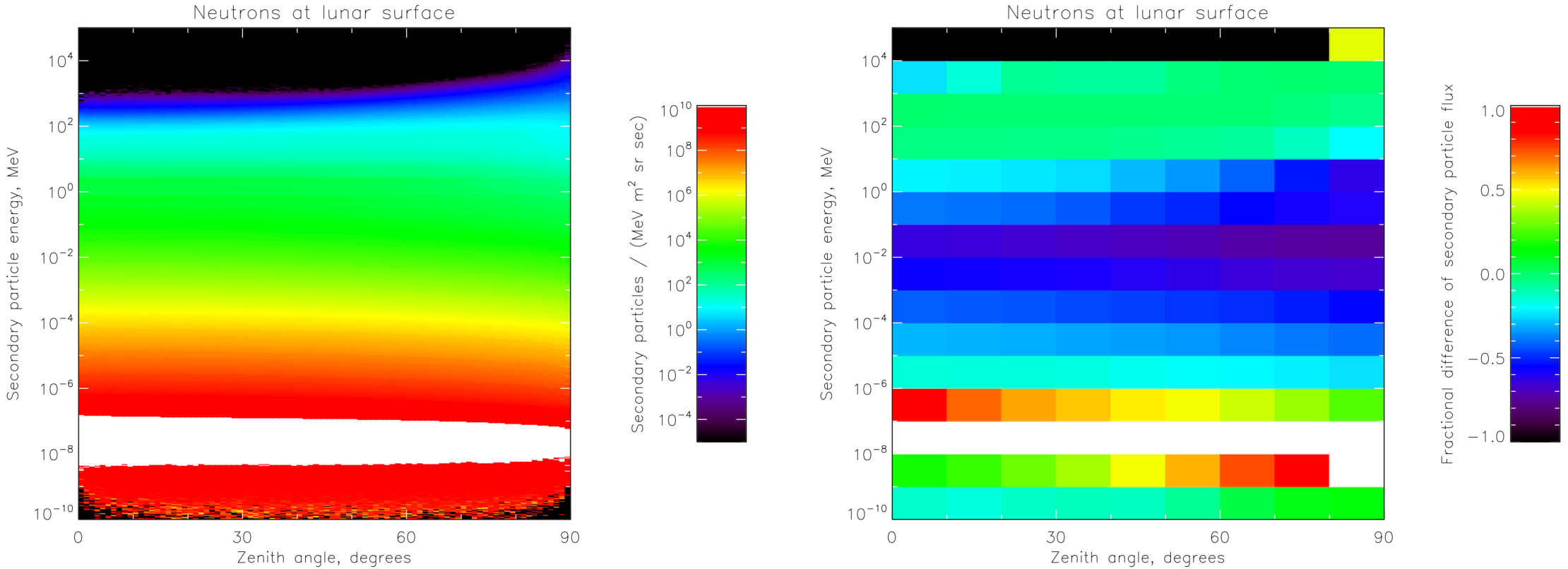

Likewise, in the first iteration of this calculation neutrons were only tabulated down to 0.1 MeV. The neutron distribution corresponding to the conditions on the previous slide for protons suggests that neutrons around 1 MeV and below are efficiently transferring their energy to the protons in the hydrogenated layer; increased flux down to thermal energies is the result of this transfer, with the neutrons being “moderated” by the hydrogen in the upper layer.

Energy/Angle/Depth Distributions of Proton and Neutron Sources

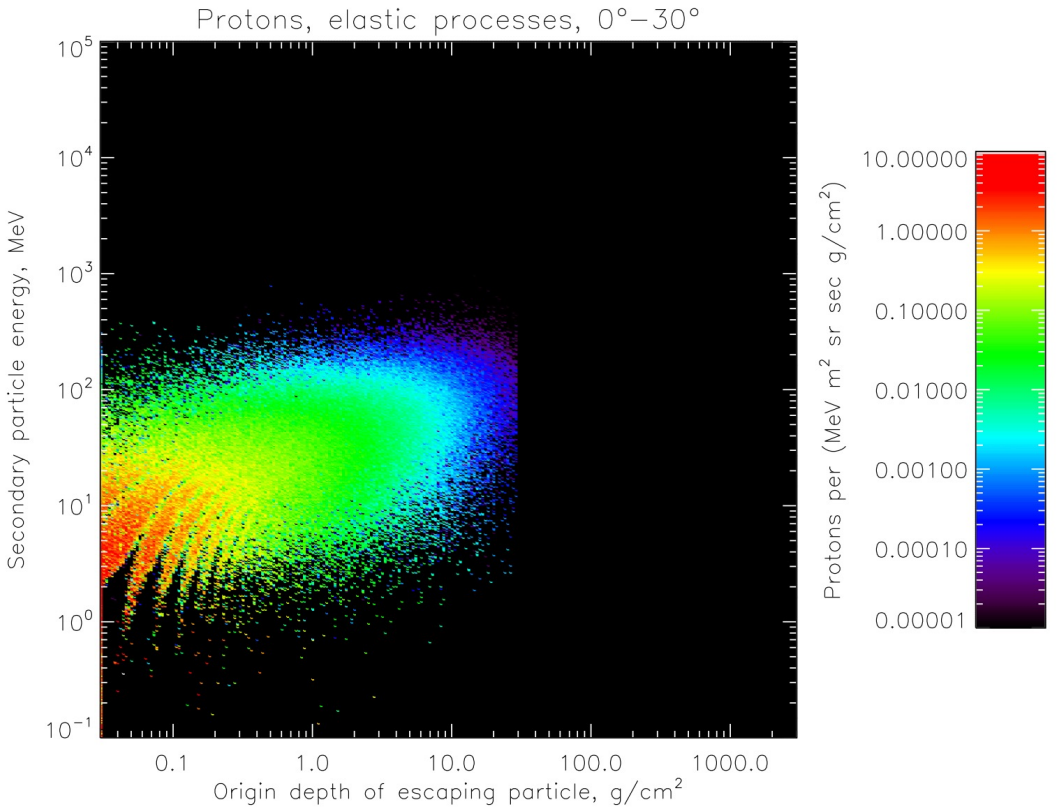

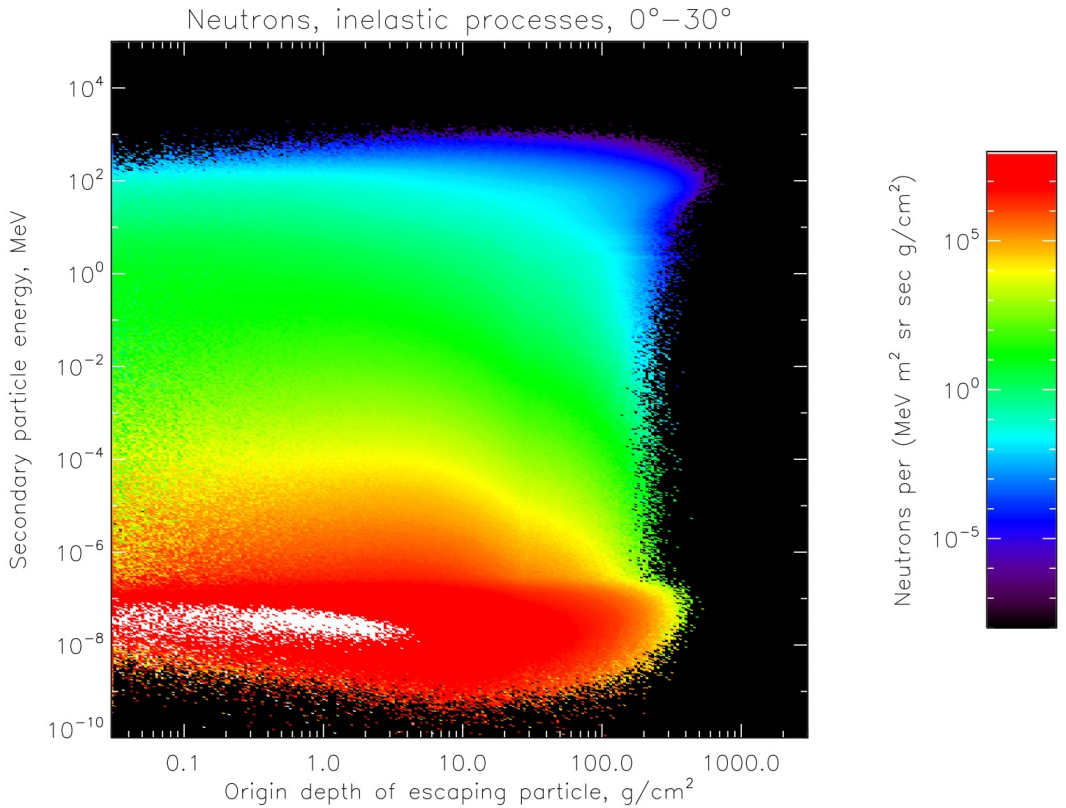

As a secondary component of the GLACE model, kernel files are also available for protons and neutrons escaping the lunar surface with the energy/angle flux also differentiated by depth of origin (and with three broad angular bins rather than 90). These are further subdivided into protons and neutrons with origins in inelastic nuclear processes and protons originating in elastic processes, almost all with neutrons from below striking protons in the hydrogenated layer. Above shows example plots for elastic protons and inelastic neutrons, energy vs. depth of origin for 10 cm layer with 1% H. Note cutoff of elastic protons at this depth (3.0 g/cc density -> 30 g/cm2 depth). Stripes are an artifact of roundoff during tracking, and do not change totals.

Effects of Solar Modulation of Incident Cosmic-Ray Ion Spectra

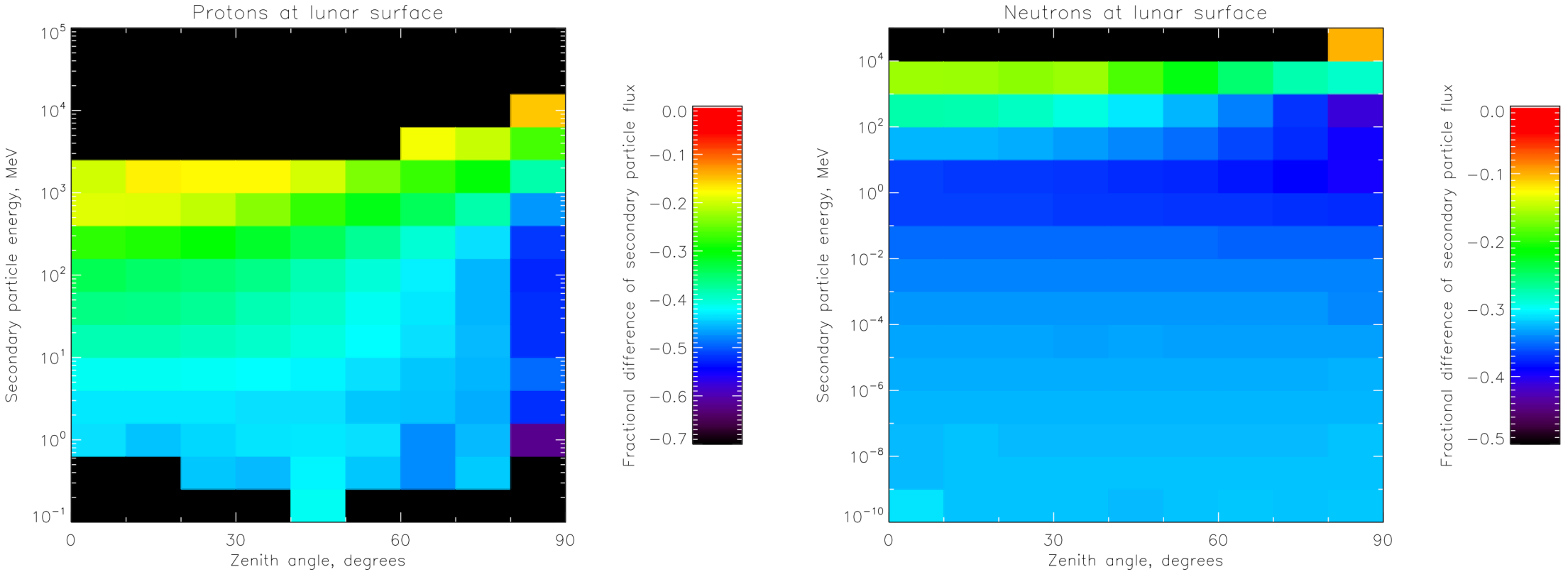

These plots show the fractional change (all negative) when kernels for protons and neutrons produced from dry FAN are convolved with incident ion spectra corresponding to solar maximum modulation rather than solar minimum as on the previous slides. This is noticeably bigger than the magnitude of changes on, e.g., slide 6 for protons in the CRaTER energy range (tens of MeV), indicating that we will need to be careful to separate solar-cycle effects from our mapping of those observations; however, changes at lower energies due to presence of hydrogen should still stand out, though correction will be necessary.

Proton Fluxes Projected from 0 to 20 km Altitude vs. Tabulated There

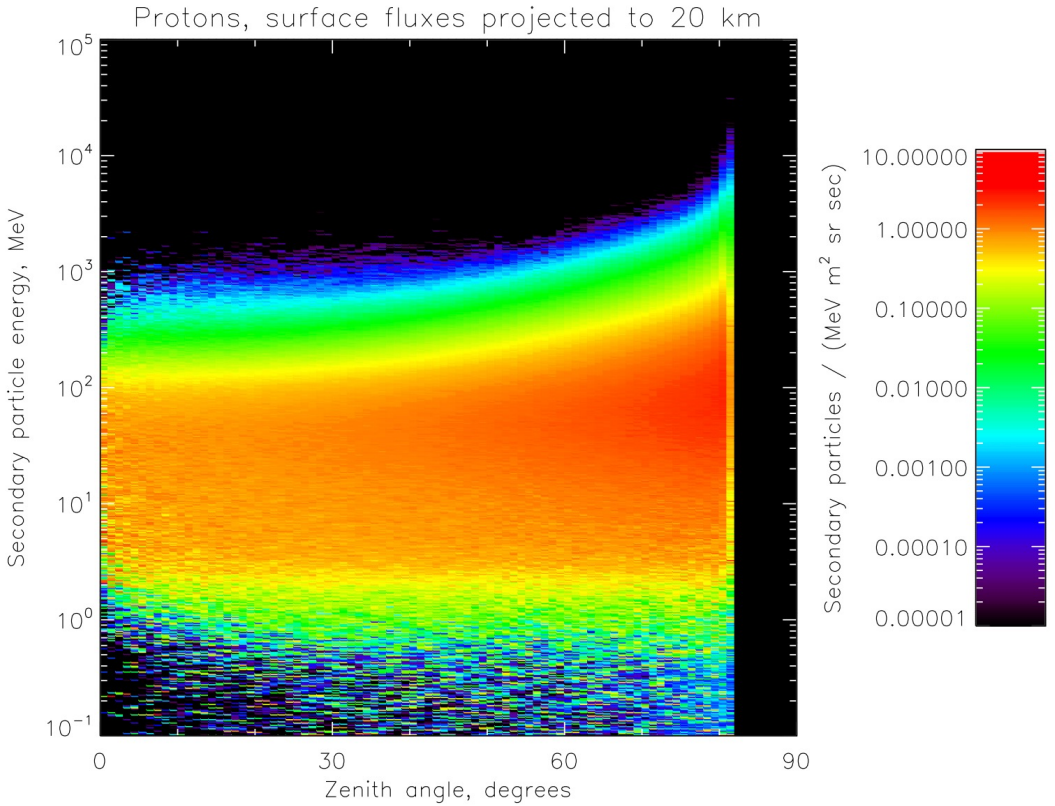

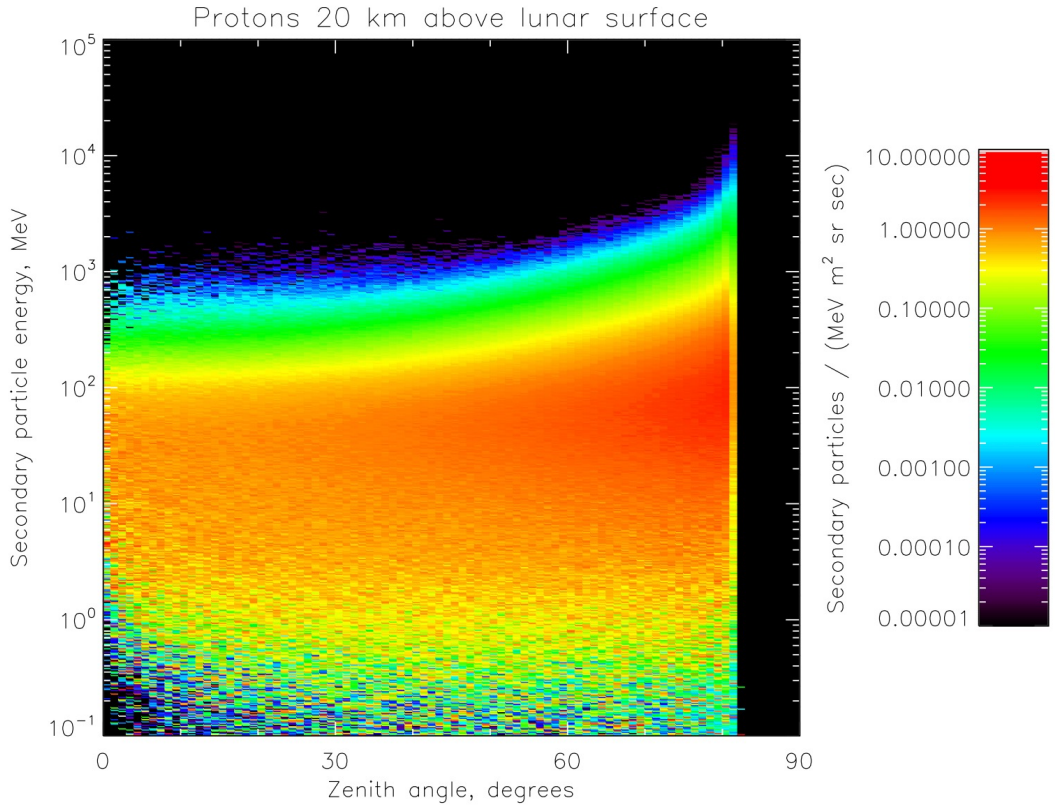

Albedo particles are tabulated at 20 km altitude as well as at the surface in order to account for decay of unstable ones on the way up (e.g., all pions and almost all muons). We can trigonometrically project fluxes from surface to 20 km altitude, as at left; e.g, since the Moon subtends a half-angle of 81.3° at 20 km, the horizon flux (90°) at the surface projects to 81.3° in the plot at left, with no flux beyond that angle. At right is the flux tabulated directly at 20 km; there is some enhancement around 1 MeV, which will complicate analysis of the excess noted on slide 6 due to surface hydrogenation, but the cutoff is still sharp at the limb. (Dry FAN, solar minimum.)

Positron Fluxes at 20 km Altitude

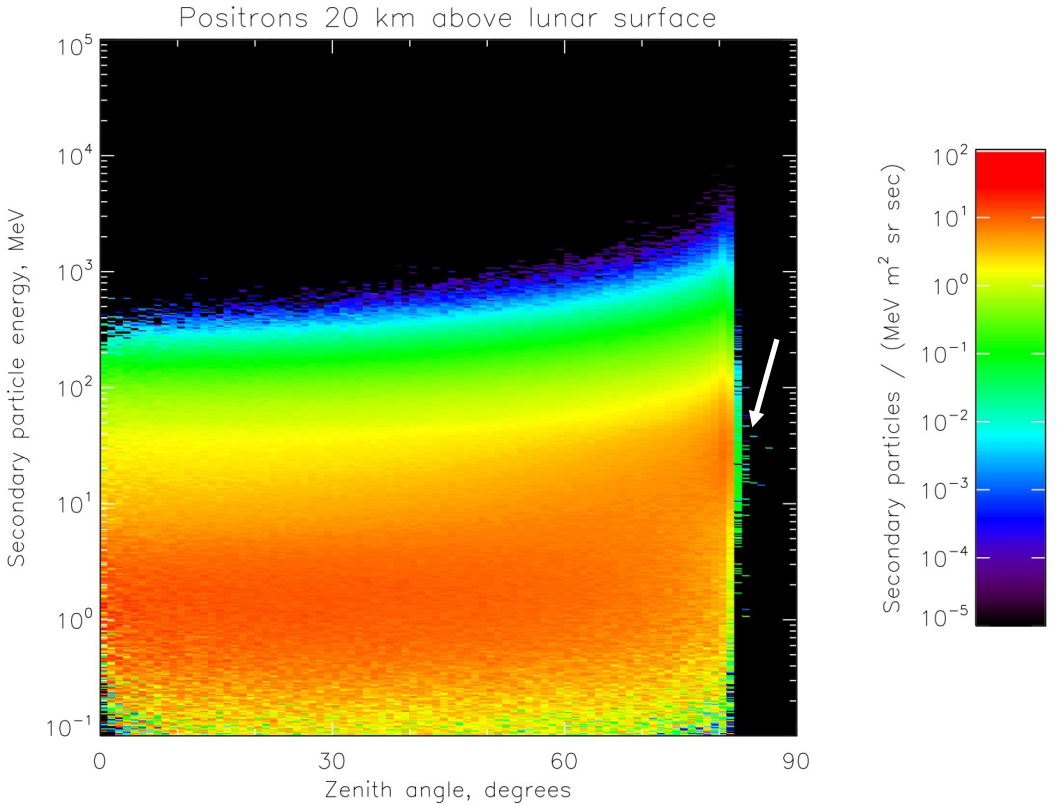

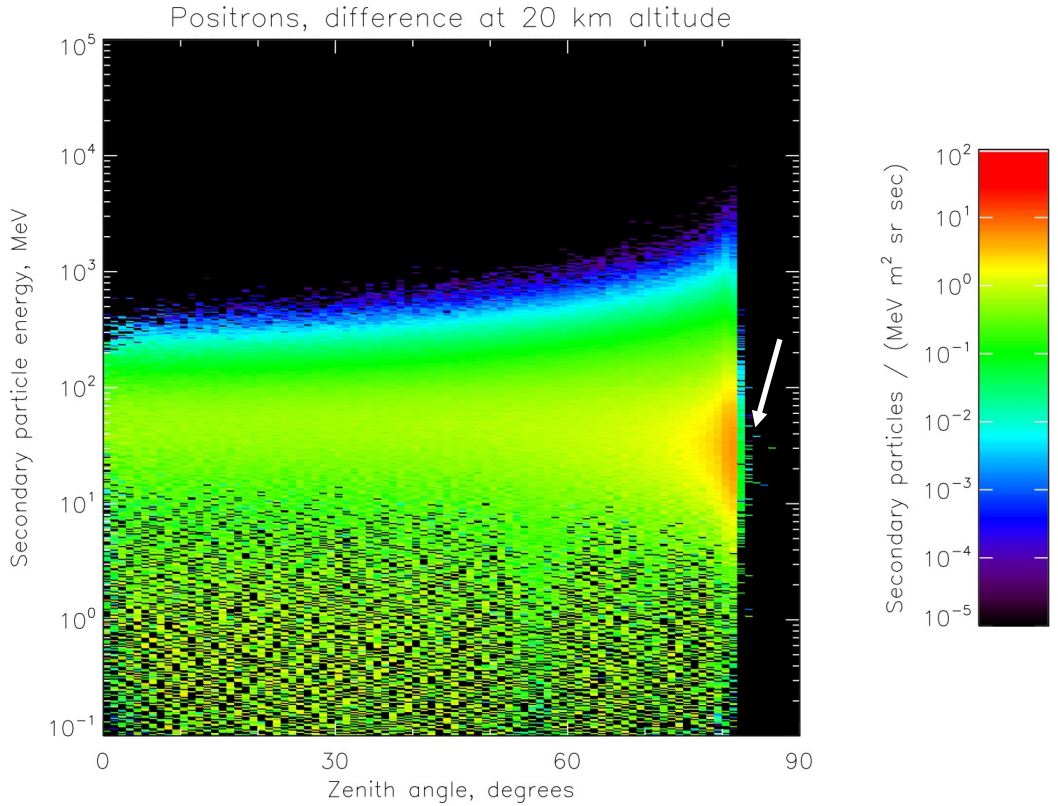

At left are the positron fluxes tabulated at 20 km altitude, and at right is the difference between that distribution and the surface distribution projected to 20 km altitude as on the previous slide. Note small amount of flux (arrowed) beyond the limb at 81.3°; these are positrons produced from, e.g., muons that are headed just off from the point of observation but that, upon decaying below 20 km, create an electron that is deflected just enough to reach that observation point, thus appearing to come from beyond the lunar limb.

Electron Fluxes at 20 km Altitude

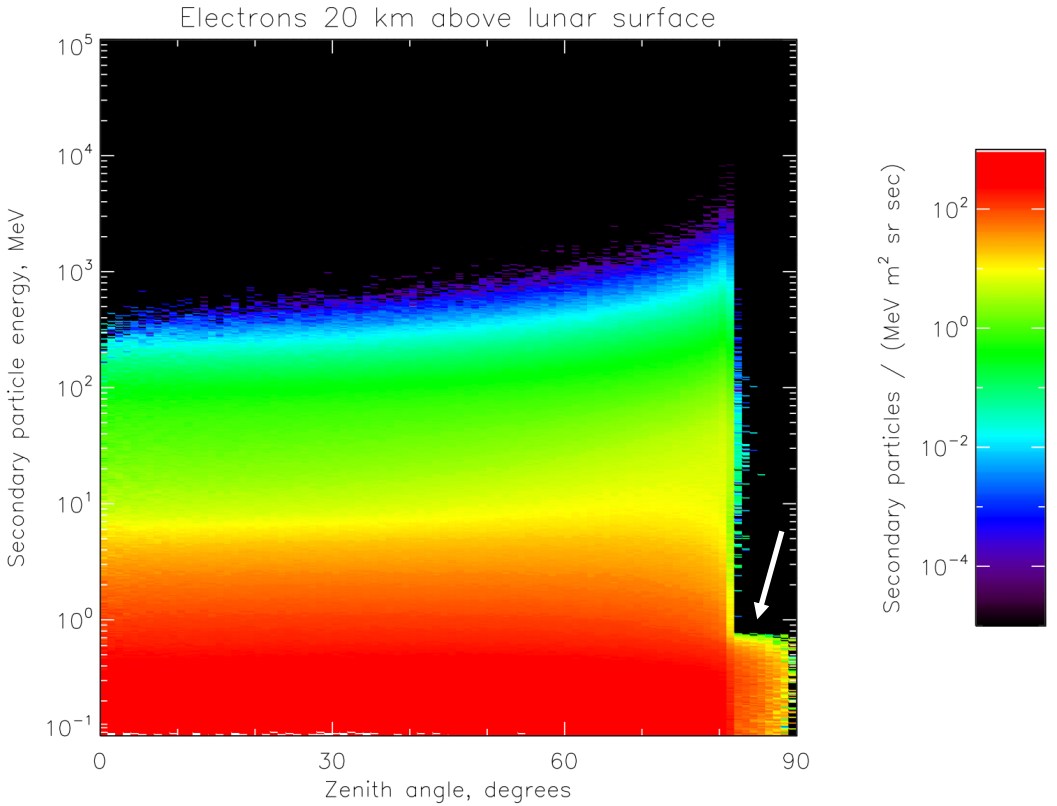

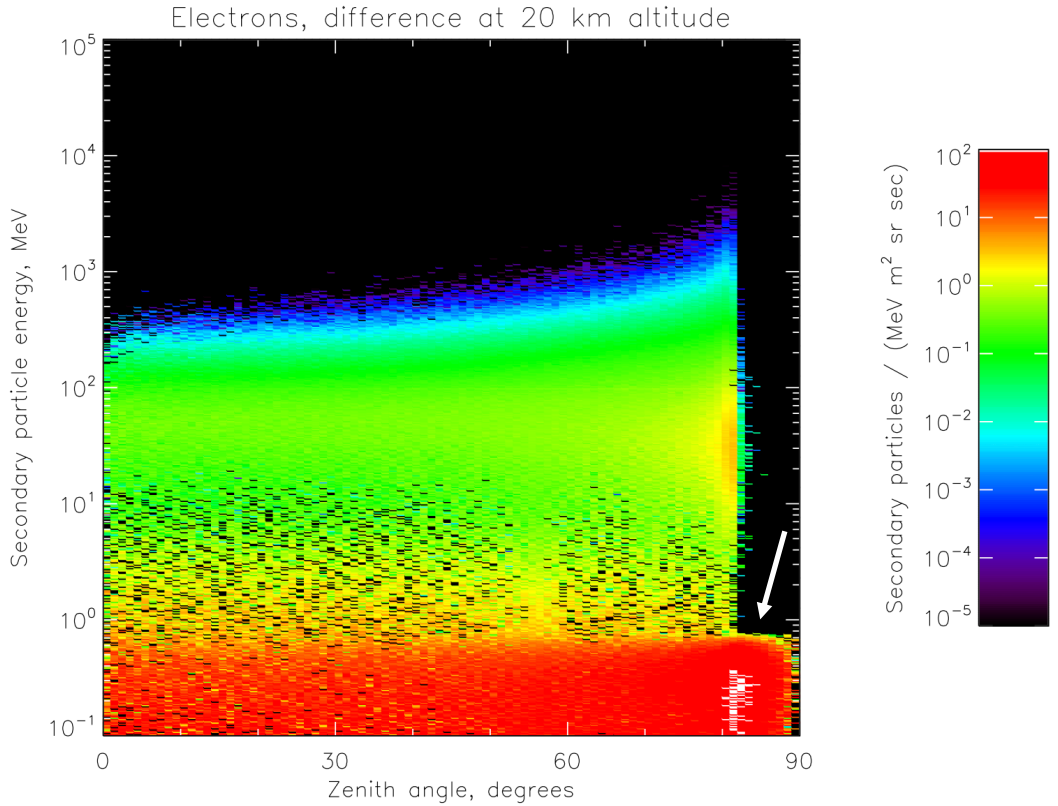

For electrons, however, in addition to the decays of energetic particles that transfer most of their momentum to the electrons (so that they deviate only slightly from the primary particle's path), we also see a broad, nearly isotropic band of electrons at low energies (arrowed), going well past the limb. These are from the decay of neutrons, which gives a cutoff at 0.78 MeV. Since most decaying neutrons have low energies, their product electrons are produced nearly isotropically, and may come from well off to the sides of, or even above, the point of observation at 20 km! (We are missing those that would be seen from 90° to 180°.)

Neutron Electron Water Tomography (NEWT)

- The previous slide suggests a new way to prospect for water at or near the lunar surface: measure the electrons resulting from the decay of water-modulated neutrons.
- Advantage: electron sensors are much simpler than neutron sensors. E.g., neutron-decay electrons at Earth were first identified using a sensor aboard the CSSWE CubeSat (Li et al., 2017), and their energy spectrum was confirmed to match the beta-decay shape using an even simpler (passively collimated single detector) sensor aboard DEMETER (Zhang et al., 2019).
- Disadvantage: mapping water on the lunar surface would be a complex tomography-inversion problem, since electrons coming from a given direction could be produced from a neutron decaying anywhere along a line from the sensor in that direction. The point of surface escape (vs. the point of decay) of the neutron would be even more ambiguous, with trajectories having to be modeled in the presence of gravity (e.g., a thermal neutron traveling straight up would turn and start to fall back around 20 km altitude).
- Complication: a directional electron telescope looking away from the lunar limb (including straight up) would not sense albedo electrons from the surface, but would be subject to background signals of similar intensity, e.g., Jovian electrons. Spectral shapes could be used to distinguish these from neutron decay.
- Possible simple application: a single telescope on the surface, looking straight up, could monitor the effects of suspected diurnal variations in hydrogen content near the surface in a given region.

Ongoing Work

- The primary impetus for developing this model was to understand CRaTER albedo proton observations at several tens of MeV. Comparisons of model predictions and observations are underway.
- Others have modeled albedo particles, especially neutrons, and there are observations of global lunar photon and neutron spectra. We will compare our model results with those.
- Protons and neutrons are modulated much more by the presence of hydrogen in the regolith at lower energies than we had examined previously. This could be exploited to propose sensors better suited to remote sensing of water than, e.g., CRaTER, whose albedo proton response is serendipitous. This could include applying the NEWT technique to use electrons to probe bulk (thermal) neutron production and modulation.
- Zaman et al. (2022) compared lunar cosmic-ray albedo as modeled by five different Monte Carlo codes, including Geant4, finding that results for dry regolith were consistent across codes (that is, results in GLACE are not likely to be idiosyncratic to Geant4). A similar comparison using simulations of albedo from regolith with water intermixed is in progress.
- Further progress will be discussed in December at the Geant4 Space Users Workshop and Fall AGU Meeting, and two journal articles are in preparation.
- A comprehensive README file is available from the GLACE webpage, doi: 10.5281/zenodo.8343472

References

- Allison, J., et al., “Recent Developments in Geant4,” *Nucl. Instrum. Meth. A* **835**, 186-225 (2016), DOI: 10.1016/j.nima.2016.06.125
- Li, X., et al., “Measurement of Electrons from Albedo Neutron Decay and Neutron Density in Near-Earth Space,” *Nature* **552**, 382-385 (2017), doi: 10.1038/nature24642
- Looper, M. D., et al., “The Radiation Environment Near the Lunar Surface: CRaTER Observations and Geant4 Simulations,” *Space Weather* **11** (4), 284-296 (2013), doi: 10.1002/swe.20043
- Slaba, T. C., and K. Whitman, “The Badhwar-O’Neill 2020 GCR Model,” *Space Weather* **18** (6), e2020SW002456 (2020), doi: 10.1029/2020SW002456
- Zhang, K., et al., “Cosmic Ray Albedo Neutron Decay (CRAND) as a Source of Inner Belt Electrons: Energy Spectrum Study,” *Geophys. Res. Lett*. **46** (2), 544-552 (2019), doi: 10.1029/2018GL080887